Short Article

Factors Limiting the Frequency of RTD Oscillators

Dinh-Tuan Nguyen, Hoang-Gia Vu

Faculty of Radio-Electronic Engineering (FREE), Le Quy Don Technical University, 236 Hoang Quoc Viet, Hanoi, Vietnam

Correspondence: Dinh-Tuan Nguyen, tuannd_hv@lqdtu.edu.vn
Communication: received 08 April 2026, revised 01 June 2026, accepted 11 June 2026
Online publication: 23 June 2026, Digital Object Identifier: 10.21553/rev-jec.461

***Abstract*– Availability of room temperature, high output power, compact and coherent sources is a critical factor for many applications in the THz frequency range. Resonant-tunneling-diode (RTD) oscillators are one of the best choices for these purposes. While the basic principles of RTD oscillators are known, there is a lack of quantitative analysis regarding how frequency-dependent spreading resistance and specific contact parasitics collectively limit the practical oscillation frequency in slot-antenna configurations. This paper provides a comprehensive equivalent circuit model that integrates frequency-dependent spreading resistance and contact parasitics to define the exact mesa area and antenna dimensions required to maximize the oscillation frequency for a specific RTD wafer.**

***Keywords*– RTD oscillators, slot antenna, spreading resistance, contact parasitics, THz electronics.**

1 Introduction

Resonant-tunneling-diode (RTD) oscillators are among the most promising types of THz sources for practical applications. [1, 2]. They are simple, compact (could be smaller than mm^2), [3] with high DC-to-THz conversion efficiency ($\approx 5\,\%$ at 0.1 THz and $\approx 1.5\,\%$ at ≈ 0.5 THz), [4, 5] work at room temperature, can provide high output power (≈ 10 mW at 0.45 THz in array configuration), [6] and can cover frequencies up to almost 2 THz. [7] To achieve higher frequencies and improve the performance of RTD oscillators in the THz range, one needs to reduce the oscillator losses. [1, 2] The losses have two main sources. One of the losses that are related to losses is in the resonator/antenna of an RTD oscillator. The other source of losses are the parasitics of the RTD itself. The main contribution to parasitics comes from the RTD contact resistance, the spreading resistance.

An ac equivalent circuit of an RTD oscillator is sketched in Figure 1. The oscillator consists of an RTD, an antenna, and parasitic elements. The complex ac admittance of the RTD can be represented, without loss of generality, as an RC circuit, where the real and imaginary parts of the admittance are represented by a resistor (with conductance $g_{RTD}A$) and a capacitor ($c_{RTD}A$), respectively. Here, A is the RTD area, g_{RTD} and c_{RTD} are, respectively, the specific (per unit area) RTD conductance and capacitance. g_{RTD} and c_{RTD} are, generally speaking, dependent on frequency (we denote the fundamental angular oscillation frequency as ω) and, non-linearly, on ac voltage. C_{par} represents the parasitic capacitance of the RTD, which is connected in parallel with the antenna admittance Y_a. The reason for this arises from the electrical coupling between the RTD mesa structure and the surrounding antenna/electrode metallization.

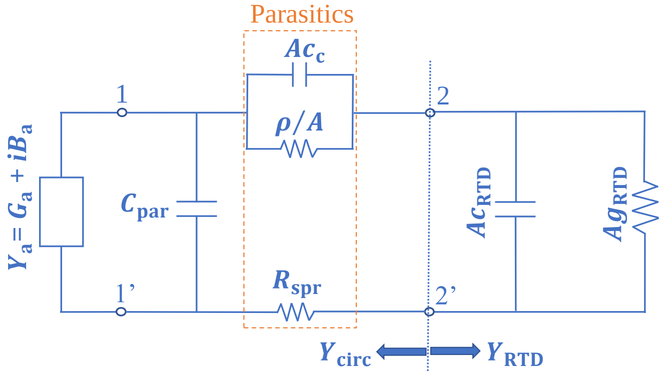

Figure 1. Ac equivalent circuit of an RTD oscillator.

The oscillator consists of two main parts: (i) the RTD as a source of spontaneous oscillations; (ii) slot antenna as the radiator and resonator that defines the fundamental frequency of the oscillator. The RTD requires DC biasing to bring it into the oscillation region. A conductive bridge over the slot is needed to grant that the RTD mesa top electrode and the opposite side of the antenna, where the bias is applied, are connected (see Figure 2). Also, to separate the DC biasing circuit from the ac circuit of the oscillator, a metal-insulator-metal (MIM) structure is required. In addition, a shunt resistor is needed to suppress low-frequency parasitic oscillations in external circuits including the bias line.

In order to make RTD oscillators working, the condition: $|G_{RTD}| > G_a$ must be satisfied, where G_{RTD} and G_a are the conductance of RTD and antennas. RTD oscillators stop working when RTD cannot provide enough NDC to compensate for the resonator losses or RTD cannot provide any gain at all beyond certain limiting frequencies, since NDC turns into PDC with increase of frequency. (NDC is defined as Negative Differential Conductance, and PDC as Positive Differential

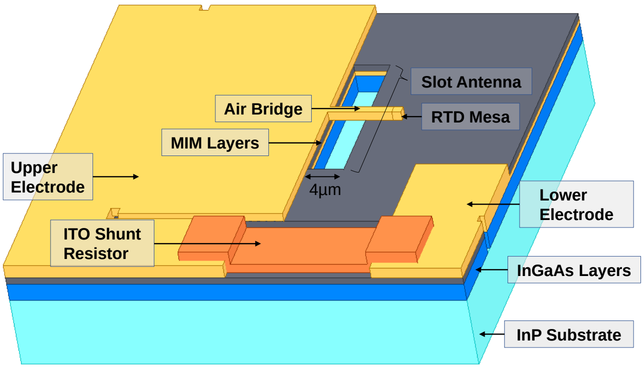

Figure 2. Structure of the proposed design. The RTD is situated in the center of the right side of the slot antenna.

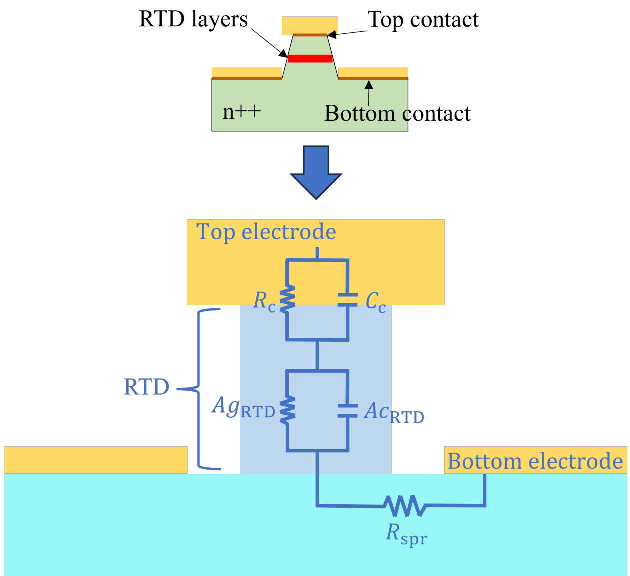

Figure 3. Cross-section of the physical RTD connection to the circuit and the corresponding equivalent circuit.

Conductance). The maximum oscillation frequency of an RTD oscillator is limited by parasitic elements and by RTD parameters themself. In this paper, we explicitly investigate the impact of two primary factors: (1) specific contact resistance (R_c) and (2) frequency-dependent spreading resistance (R_{spr}) within a basic slot-antenna configuration. None of the above contributions is working independently, they are coupled due to the concept of the RTD oscillators. However, we can define the effect of each factor on the RTD oscillators when its parameters are considered predominate. The upper limitation of the oscillation frequency of an RTD oscillator can be defined based on the oscillation conditions.

2 Impact of the contact's parasitics

Figure 3 shows the cross-section of the physical RTD connection to the circuit. The connectivity between the RTD layers and the circuit is established via semiconductor layers, which are subsequently interfaced with deposited metallic layers. The interface between a semiconductor and a metal results in the manifestation of contact resistance. The schematic illustration portrays the denotation of the contact resistance of the top contact as R_c. The homogeneity of the current along the top contact results in an inverse relationship between the contact resistance of the top contact and its contact area as $R_c = \rho_c/A$, where ρ_c and A are the specific contact resistivity (its unit is $\Omega\mu m^2$) and the active area of the RTD (in μm^2). The interfaces of the contacts can be induced with a charge accumulation. The outcome of this phenomenon is the emergence of contact capacitance denoted as C_c, which operates in parallel with the contact resistance R_c and is directly proportional to the contact area $C_c = c_c \cdot A$, where c_c is the specific contact capacitance (in $\Omega/\mu m^2$).

The current that passes through the top contact and the RTD subsequently spreads into the severely doped semiconductor layer beneath the RTD and the metallic bottom contact. Because the current does not pass through the bottom contact uniformly in this situation, the relationship between the bottom equivalent contact resistance and the RTD area is more complicated than it is in the top contact instance. In the equivalent circuit, R_{spr} stands in for the resistance caused by current spread and scattered bottom contact resistance. Physically, the current paths also have a parasitic capacitance and inductance. Due to the RTD and its contacts' sub-micrometer scale, this inductance ordinary has a minimal impact, as seen in Reference [8]. The contact parasitic elements are linked in a sequential manner within the oscillator circuit, interconnecting the RTD and the resonator. The frequency operational region is commonly constrained by an RC time constant that arises from contact parasitics. In order to ascertain the maximum operation frequency of an RTD, it is necessary to substitute it with the corresponding small-signal equivalent circuit. This circuit comprises of a parallel connection between the RTD capacitance (C_{RTD}) and conductance (G_{RTD}), as described in Reference [2] and [8].

2.1 Typical values of the contact parasitics

The typical value of ρ_c in RTDs with InGaAs contact layers is 1-10 $\Omega\mu m^2$. Nonetheless, it is possible for the value to exceed 100 $\Omega\mu m^2$ if appropriate measures are not implemented to produce high-quality contacts. Terahertz resonant tunneling diodes (RTDs) typically feature narrow tunnel barriers, elevated current density, and pronounced negative differential conductance (NDC). In the context of RTDs, it is imperative that the working point falls within the NDC region and that the RTD exhibits DC stability in that region. This necessitates that the value of ρ_c be less than $-1/G^0_{RTD}$, where G^0_{RTD} represents the specific static differential conductance of the RTD (G^0_{RTD} is negative in the NDC region). An RTD utilized in a 1.74 THz oscillator in [9] did not exhibit a record-high peak current density of $j_{RTD} \approx 23.6$ mA/μm^2. However, it did possess a value of $1/G^0_{RTD} \approx -7.5$ $\Omega\mu m^2$.

Consequentially, it is imperative that the value of ρ_c is maintained at a level lower than -1/G^0_{RTD}, in order to effectively bias the RTD within the NDC region.

The larger area of the bottom RTD contact is typically deemed less crucial, however, its impact on the overall contact resistance of the RTD should not be disregarded. This implies that the value of ρ_c must be lower than the one determined in the aforementioned evaluation. Taking an example: the conductance and capacitance of an RTD are -50 mS/µm^2 and 12 fF/µm^2, respectively. The contact parasitics have the resistance value of 2 Ωµm^2 and the capacitance value of 20 fF/µm^2. This RTD oscillator gives us the maximum frequency of ≈ 2.3 THz. Despite the fact that this is a very rough approximation, it is pretty near to the highest achieved oscillation frequency of the RTD oscillators, which is 1.98 THz, see [7], which was received with an RTD with the same parameters.

2.2 Spreading resistance

Subsequently, we will discuss the evaluation of the spreading resistance and its impact. This contribution is a result of the propagation of electrical currents within the semiconductor conducting layer beneath, which subsequently overflow onto a segment of the lower electrode. An expression for the spreading resistance of a symmetric RTD can be derived using transmission line theory. This is typically applied to RTDs with cylindrical mesa geometry, see [10–12]. The validity of the transmission line method is contingent upon the transfer length, defined as the effective length of the contact wherein current is absorbed, being significantly greater than the thickness of the conductive layer. This assumption allows for a uniform current distribution within the semiconductor layer.

Figure 4 describes the cross-section view and the top view of the spreading resistance for a symmetric RTD coupling with a slot-antenna. We have here: r is the radial coordinate, r_1 and r_2 (in µm) are the radius of the active area of the RTD and RTD mesa cap area covering by metal, respectively (the value of $r_2 - r_1$ defines the etching depth of RTD mesa). D is the depth (typical value of it is in the range of $0.5 - 1$ µm), and σ is the conductivity (in $\frac{\text{S}}{\text{m}}$) of the doped layer beneath the RTD layers (InGaAs in this example). ϵ is the permittivity of the semi-insulating substrate layer (InP for this example). M_2 is the bottom metal contact layer which is very large in comparison with the top RTD metal contact layer. I here is the current flowing through the RTD.

In order to calculate the value of the spreading resistance, we can write the following equations

$$\mathrm{d}I = j\alpha r \mathrm{d}r. \tag{1}$$

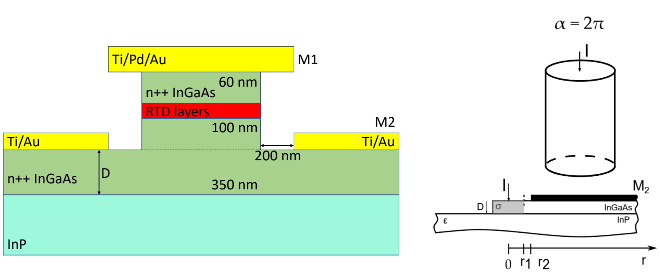

Figure 4. Cross section of an RTD contact layers.

Taking the integral for both sides of Equation 1, we have

$$I(r) = j\alpha \frac{r^2}{2}. \tag{2}$$

The electric field going in the InGaAs layer is defined as:

$$I(r) = \sigma E(r) r \alpha D \Rightarrow E(r) = \frac{1}{2}\frac{j}{\sigma D} r, \tag{3}$$

and

$$U = \int_0^{r_1} E(r) dr = \int_0^{r_1} \frac{1}{2}\frac{j}{\sigma D} r dr = \frac{1}{4}\frac{j}{\sigma D} r_1^2, \tag{4}$$

$$R = \frac{U}{I(r_1)} = \frac{1}{2}\frac{1}{\sigma D \alpha}. \tag{5}$$

The spreading resistance then is defined as following

$$R_{spr} = \sum R = \frac{R_{sh}}{\pi}\left\{\frac{1}{4} + \ln(\frac{r_2}{r_1}) + \frac{K_0(\frac{r_2}{L_T})L_T}{K_1(\frac{r_2}{L_T})r_2}\right\}, \tag{6}$$

where K_0 and K_1 are the modified Bessel functions of zero and first orders, respectively. L_T and R_{sh} are the transfer length (in µm) and the sheet resistance (in Ω):

$$L_T = \sqrt{\frac{\rho_c}{R_{sh}}}, \tag{7}$$

$$R_{sh} = \frac{1}{\sigma D}. \tag{8}$$

with ρ_c is the contact resistivity (in Ωµm^2). Taking an example as following (see Figure 4): The active area A of an RTD is 0.21 µm^2, the conductivity σ_{InGaAs} and the depth D of the n++ InGaAs layer (with doping of 3×10^{19} cm^{-3}) are 3.93×10^5 $\frac{\text{S}}{\text{m}}$ and 350 nm, respectively. The top $\rho_{c,1}$ and the bottom $\rho_{c,2}$ contact resistivity are 2 Ωµm^2 and 10 Ωµm^2, respectively. By using Equation 6, the spreading resistance R_{spr} in this case is 4.9 Ω. This value of R_{spr} is somehow comparable with Reference [13] which had R_{spr} of 4 Ω with D = 400 nm, and 2 Ω with D = 600 nm.

We should notice that all the above equations are formulated for the DC case (frequency is zero). As the frequency changes, the transfer length L_T will change, as a result the spreading resistance will also change. The dependence of the spreading resistance on the frequency (with different values of RTD area A) can be seen in the Figure 5.

From Figure 6, we can notice that both the top contact resistance and the spreading resistance decrease with increasing of frequency. For example, at DC case (frequency is zero), R_c and R_{spr} are 10 Ω and 2.84 Ω, respectively; however, these values at HF case (high frequency, for example at 2 THz) are 7.98 Ω and 2.14 Ω, respectively. In the high-frequency regime, the RTD areas of the RTD oscillators are quite small (in the range from 0.1 µm^2 to 0.5 µm^2). The spreading resistance R_{spr} of these RTD areas has small impact; however, the top contact resistance R_c plays a huge contribution on the total parasitic resistance. The spreading resistance is dominant for large RTD areas (from ∼ 1.0 µm^2 in the DC case, or from ∼ 1.2 µm^2 in the HF case).

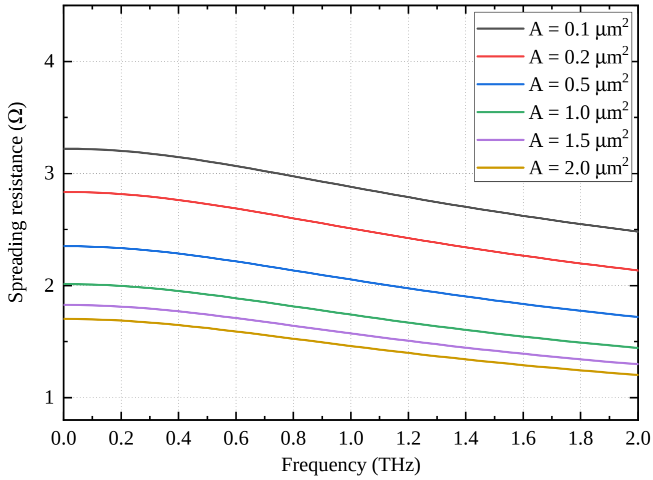

Figure 5. Dependence of the spreading resistance on the frequency with different RTD areas.

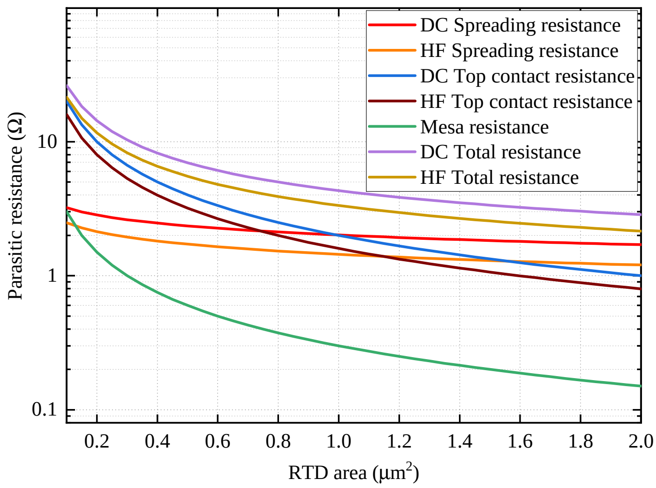

Figure 6. Comparison of the contributions of the parasitic resistances. The RTD area is from 0.1 to 2.0 μm^2. The HS case is considered as the frequency at 2 THz.

3 Frequency limitation of RTD oscillators

Next, we will introduce the impact of both contact parasitics and spreading resistance on the slot-antenna RTD oscillator to have an estimation on frequency limitation of the system. The results are calculated regarding the equivalent circuit of the RTD oscillator in Figure 1. For investigating the frequency limitation of RTD oscillators, we can only use the small-signal model for RTD conductance and capacitance, see more details in [2], [14–17].

The conductance and capacitance of the RTD are calculated as:

$$G_{RTD} = g_{RTD} \cdot A, \tag{9}$$

$$C_{RTD} = c_{RTD} \cdot A, \tag{10}$$

where g_{RTD}, c_{RTD} are the specific conductance, capacitance (per unit area), and A is the mesa area of the RTD. The admittance of the RTD and the contact parasitics are written as:

$$Y_{RTD} = G_{RTD} + i \cdot \omega \cdot C_{RTD}, \tag{11}$$

$$Y_c = \frac{1}{R_c} + i \cdot \omega \cdot C_c, \tag{12}$$

with R_c and C_c are the contact resistance and capacitance. The admittance of the circuit from the left side of the points 2-2′ in Figure 1 (including antenna, contact parasitics and spreading components) is

$$Y_{circ} = \left(\frac{1}{Y_a} + \frac{1}{Y_c} + R_{spr}\right)^{-1}, \tag{13}$$

where R_{spr} is the spreading resistance, Y_a is the antenna admittance (the parasitic RTD capacitance C_{par} is included in Y_a as a parallel capacitor to the antenna). We can then write the total admittance of the RTD oscillator as

$$Y_{total} = Y_{circ} + Y_{RTD}, \tag{14}$$

or:

$$\mathrm{Re}(Y_{total}) = \mathrm{Re}(Y_{circ}) + G_{RTD}, \tag{15}$$

$$\mathrm{Im}(Y_{total}) = \mathrm{Im}(Y_{circ}) + \omega \cdot C_{RTD}. \tag{16}$$

The oscillation condition is satisfied when $\mathrm{Im}(Y_{total}) = 0$, and $\mathrm{Re}(Y_{total}) <= 0$. The data for Figure 7 and Figure 8 were obtained by numerically sweeping the frequency ω for various RTD areas A and antenna lengths L until the conditions above were violated.

Figure 7 shows the dependence of the frequency limitation of the slot-antenna RTD oscillator on the RTD area with different values of the contact resistivity ρ_c from 1 to 10 Ωμm^2, The RTD specific contact capacitance c_c is taken as 19 fF/μm^2, and the parasitic RTD capacitance C_{par} is assumed ∼ 1 fF/μm^2. In this example, only the contact parasitics are taken into account of the system. The width of the slot antenna is 4 μm, and the length varies from 12 to 100 μm. The RTD in this case has 1.6 nm thick barrier with the peak current density of around 6 mA/μm^2. The points in the brackets show the RTD area and the maximum oscillation frequency that the RTD oscillator can achieve with certain value of the contact resistivity. The highest oscillation frequency in this case is about 732 GHz on the RTD oscillator with 1.5 μm^2 RTD, 20 μm slot-antenna length, and the contact resistivity 1 Ωμm^2.

The simulations utilize a fixed slot width of 4 μm, which is a standard dimension in THz lithography to balance radiation efficiency with manageable parasitic inductance. If the slot width is modified, the antenna admittance Y_a will change, shifting the resonance points. However, the general conclusion—that an optimal RTD area exists for maximizing frequency - remains valid despite these absolute value shifts.

The spreading resistance now is also taken into the system together with the contact parasitics. As can be seen from Figure 8, the maximum oscillation frequencies of the RTD oscillator decrease a lot in comparison with the above case when only the contact parasitics are involved in the system. The highest oscillation frequency in this case is about 480 GHz on the RTD oscillator with 1.5 μm^2 RTD, 50 μm slot-antenna length, and the contact resistivity 1 Ωμm^2.

Figures 7 and 8 also show that for small RTD areas (in the range of 1 μm^2), the maximum oscillation frequencies change not much (correspond to the antennas with lengths 75 μm and 100 μm). In this RTD area range, as discussed above, the contact resistance is dominant over the spreading resistance, see Figure 6. For the larger RTD areas, where the impact of the spreading resistance is dominant, the maximum oscillation frequencies decrease a lot in the case when the spreading resistance is employed to the system (Figure 8).

Based on the results represented in Figure 8, one can define the antenna parameters (length and width) and the RTD area in order to achieve the highest oscillation frequencies of the slot-antenna RTD oscillator on certain contact resistivity for a given RTD wafer. However, together with maximizing oscillation frequencies, achieving high output powers of the RTD oscillators is also important.

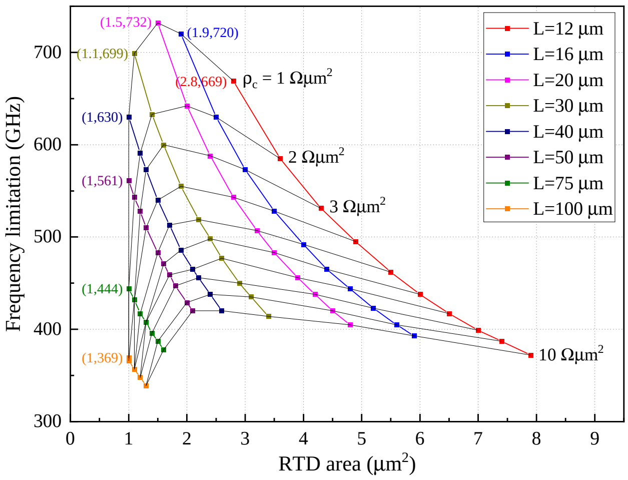

Figure 7. The dependence of the frequency limitation of the slot-antenna RTD oscillator on the RTD area with different contact resistivity. Only the contact parasitics are taken into account in this case.

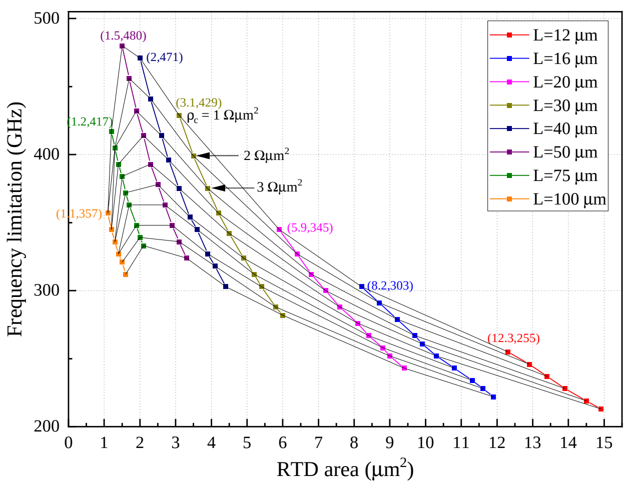

Figure 8. The dependence of the frequency limitation of the slot-antenna RTD oscillator on the RTD area with different contact resistivity. The contact parasitics and spreading resistance are taken into account in this case.

In comparison with other oscillators in Table I. The frequency limits reported here (e.g., 732 GHz for $\rho_c = 1$ Ωμm^2 in Figure 7) are lower than record values like 1.98 THz. This is primarily because our model utilizes a moderate current density RTD (≈ 6 mA/μm^2) rather than record-high 23.6 mA/μm^2 devices. Furthermore, we rigorously include R_{spr}, which significantly penalizes the frequency limit.

Table I
Comparison of Slot-Antenna RTD Oscillators

References	Frequency (GHz)	W–L (μm)	RTD oscillator type
Current work	480–732	4–(12–100)	Slot antenna
Reference [5]	400–600	4–(50,100)	Slot antenna
Reference [4]	530–590	4–130	Slot antenna
Reference [7]	1980	4–9	Slot antenna

4 Conclusion

This paper investigates the primary factors that limit the maximum oscillation frequency of RTD oscillators: contact parasitics, spreading resistance, and antenna losses. Taking into account these coupled parasitic elements, we established a methodology to define optimal slot antenna dimensions and RTD mesa areas to maximize frequency for any given wafer.

References

[1] M. Asada and S. Suzuki, "Room-Temperature Oscillation of Resonant Tunneling Diodes Close to 2 THz and Their Functions for Various Applications," *Journal of Infrared, Millimeter, and Terahertz Waves*, vol. 37, pp. 1185–1198, 2016.

[2] M. Feiginov, "Frequency Limitations of Resonant-Tunnelling Diodes in Sub-THz and THz Oscillators and Detectors," *Journal of Infrared, Millimeter, and Terahertz Waves*, vol. 40, pp. 365–394, 2019.

[3] M. Feiginov, C. Sydlo, O. Cojocari, and P. Meissner, "High-Frequency Nonlinear Characteristics of Resonant-Tunnelling Diodes," *Applied Physics Letters*, vol. 99, p. 233506, 2011.

[4] M. Shiraishi, H. Shibayama, K. Ishigaki, S. Suzuki, M. Asada, H. Sugiyama, and H. Yokoyama, "High Output Power (∼400 μW) Oscillators at Around 550 GHz Using Resonant Tunneling Diodes with Graded Emitter and Thin Barriers," *Applied Physics Express*, vol. 4, no. 6, p. 064101, 2011.

[5] C. Spudat, P. Ourednik, G. Picco, D. T. Nguyen, and M. Feiginov, "Limitations of Output Power and Efficiency of Simple Resonant-Tunneling-Diode Oscillators," *IEEE Transactions on Terahertz Science and Technology*, 2023.

[6] Y. Koyama, Y. Kitazawa, K. Yukimasa, T. Uchida, T. Yoshioka, K. Fujimoto, T. Sato, J. Iba, K. Sakurai, and T. Ichikawa, "A High-Power Terahertz Source Over 10 mW at 0.45 THz Using an Active Antenna Array With Integrated Patch Antennas and Resonant-Tunneling Diodes," *IEEE Transactions on Terahertz Science and Technology*, vol. 12, no. 5, pp. 510–519, 2022.

[7] R. Izumi, S. Suzuki, and M. Asada, "1.98 THz Resonant-Tunneling-Diode Oscillator with Reduced Conduction Loss by Thick Antenna Electrode," in *Proceedings of the 42nd International Conference on Infrared, Millimeter, and Terahertz Waves (IRMMW-THz)*, 2017, pp. 1–2.

[8] M. Asada, S. Suzuki, and N. Kishimoto, "Resonant Tunneling Diodes for Sub-Terahertz and Terahertz Oscillators," *Japanese Journal of Applied Physics*, vol. 47, no. 6, pp. 4375–4384, 2008.

[9] D. T. Nguyen, P. Ourednik, and M. Feiginov, "Island THz On-Chip Slot-Antenna Resonant-Tunneling-Diode Oscillators," *Applied Physics Letters*, vol. 123, no. 4, 2023.

[10] G. Reeves, "Specific Contact Resistance Using a Circular Transmission Line Model," *Solid-State Electronics*, vol. 23, no. 5, pp. 487–490, 1980.

[11] G. K. Reeves and H. B. Harrison, "Obtaining the Specific Contact Resistance from Transmission Line Model Measurements," *IEEE Electron Device Letters*, vol. 3, no. 5, pp. 111–113, 1982.

[12] D. K. Schroder, *Semiconductor Material and Device Characterization*. John Wiley & Sons, 2015.

[13] H. Kanaya, T. Maekawa, S. Suzuki, and M. Asada, "Structure Dependence of Oscillation Characteristics of Resonant-Tunneling-Diode Terahertz Oscillators Associated with Intrinsic and Extrinsic Delay Times," *Japanese Journal of Applied Physics*, vol. 54, no. 9, p. 094103, 2015.

[14] M. N. Feiginov, "Does the Quasibound-State Lifetime Restrict the High-Frequency Operation of Resonant-Tunnelling Diodes?" *Nanotechnology*, vol. 11, p. 359, 2000.

[15] M. N. Feiginov, "Effect of the Coulomb Interaction on the Response Time and Impedance of the Resonant-Tunneling Diodes," *Applied Physics Letters*, vol. 76, p. 2904, 2000.

[16] M. N. Feiginov, "Displacement Currents and the Real Part of High-Frequency Conductance of the Resonant-Tunneling Diode," *Applied Physics Letters*, vol. 78, p. 3301, 2001.

[17] P. Ourednik, G. Picco, D. T. Nguyen, C. Spudat, and M. Feiginov, "Large-Signal Dynamics of Resonant Tunneling Diodes," *Journal of Applied Physics*, vol. 133, no. 1, p. 014501, 2023.

Dinh-Tuan Nguyen received the B.S. and M.S. degrees in Applied Mathematics and Physics from Moscow Institute of Physics and Technology, Russia in 2010 and 2012, respectively. During 2013-2018, and from 2023 until now, he has been a lecturer in Le Quy Don Technical University, Hanoi, Vietnam. Since 2018, he has been a PhD candidate in Department of Electrical Engineering and Information Technology, TU Wien, Austria. His research interests include THz electronics, sub-THz/THz resonant-tunneling-diode (RTD) oscillators, and slot antennas.

Hoang-Gia Vu received the B.E. and M.E. degrees in Electrical Engineering from Le Quy Don Technical University , Vietnam in 2007 and 2010, respectively. He received the PhD degree in Computer Engineering from Nara Institute of Science and Technology, Japan in 2018. He is currently a lecturer and a researcher at the Faculty of Radio-Electronics, Le Quy Don Technical University. His research interests include embedded systems, reconfigurable computing, parallel computing, and processor architecture.